

Electrochemical Characterization of a Martensitic Stainless Steel

A. Fattah-alhosseini *

Faculty of Engineering, Bu-Ali Sina University, Hamedan 65178-38695, Iran

Abstract

This paper focused on the characterization of electrochemical behavior of a martensitic stainless steel in the acidic solutions. For this purpose, electrochemical parameters were derived from potentiodynamic polarization, Mott Schottky analysis and electrochemical impedance spectroscopy (EIS) techniques. The potentiodynamic polarization results showed that corrosion current density of AISI 420 stainless steel was decreased with the decrease in the concentration of solution. EIS studies also showed that as concentration was decreased, the measured value of polarization resistance was increased. This trend was due to the decrease in the corrosion current density, which corresponded to potentiodynamic polarization curves. Mott Schottky analysis revealed that passive films behaved as n-type and p-type semiconductors at potentials below and above the flat band potential, respectively. Also, Mott Schottky analysis indicated that the donor and acceptor densities were increased with solution concentration.

Keywords: Martensitic stainless steel; Passive film; Mott-Schottky.

1. Introduction

Martensitic stainless steels are mainly used for applications where high strength is required. However, due to their low chromium content, they are relatively sensitive to corrosion¹⁻⁵.

The corrosion resistance of stainless steel is due to the presence of passive films formed on the surface. Generally, the substrate (the nature and content of alloying elements), the environment (aerated, deaerated, neutral, acidic or alkaline) and also, specific experimental conditions (e.g. anodic polarization) affect both the chemical composition and the structure of the passive layer⁶⁻⁸.

The passive films are mainly made up of metallic oxides or hydroxides recognized as semiconductors. Consequently, semiconducting properties are often observed on the surfaces of the passive metals⁹⁻¹². To obtain a better knowledge of passive films formed on stainless steels, many studies have been carried out to address semiconducting properties through Mott-Schottky analysis¹³. For example, Mott-Schottky analysis has been widely used to study and characterize the semiconducting properties of passive films on stainless steels¹⁴. Passivity of stainless steel is usually attributed to the formation

of a mixture of iron and chromium oxide film with a semiconducting behavior on the metal surface. In recent years, the increasing number of studies on the electronic properties of passive films formed on stainless steels has led a better understanding of the corrosion behavior of these alloys¹⁵⁻¹⁸.

Generally, chemical composition of passive films varies with alloy composition and the pH of the solution, while it is expected to affect semiconducting properties of the film^{19,20}. In basic solutions, the main effect of increasing pH on film formation is thickening the passive film, basically because iron oxides are more stable in alkaline solutions²¹. Conversely, in acid solutions, a chromium-rich oxide film is formed due to the slower dissolution of chromium oxide when compared to iron oxide²².

The present work was designed to obtain a better knowledge of the electrochemical behavior of a martensitic stainless steel in acidic solutions. The aim of this study was to investigate the influence of solution concentration on the electrochemical behavior of AISI 420 using the potentiodynamic polarization and EIS. Also, Mott-Schottky analysis was performed and the defects in concentrations were calculated.

2. Experimental procedures

The chemical composition of AISI 420 used in the present investigation is shown in Table 1. All samples were polished up to 2000 grit and mounted by cold curing epoxy resin. The samples were then degreased with acetone, rinsed in distilled water and dried with

* Corresponding author

Tel: +98 916 1620892

Fax: +98 811 8257400

E-mail: a.fattah@basu.ac.ir

Address: Faculty of Engineering, Bu-Ali Sina University, Hamedan 65178-38695, Iran

Assistance Professor

air just before each test. Aerated sulfuric acidic solutions with four different concentrations (1.00, 0.50, 0.10 and 0.05 M H_2SO_4) were used as the test solutions. All solutions were made from an analytical grade of sulfuric acid (97% H_2SO_4) mixed with water. Tests were carried out at 25 ± 1 °C.

Electrochemical measurements were performed in a conventional three-electrode cell under aerated conditions. The counter electrode was a Pt plate, while the reference electrode was Ag/AgCl saturated in KCl. Electrochemical measurements were obtained using an Autolab potentiostat/galvanostat system.

Prior to electrochemical measurements, working electrodes were immersed at OCP for 1 hr to form a steady-state passive film. Potentiodynamic polarization curves were measured potentiodynamically at a scan rate of 1 mV/s starting from $-0.25 V_{Ag/AgCl}$ (vs. E_{corr}) to $1.2 V_{Ag/AgCl}$. The impedance spectra were measured in a frequency range of 100 kHz –10 mHz at an AC amplitude of 10 mV (rms). The validation of the impedance spectra was done by checking the linearity condition, i.e. measuring the spectra at AC signal amplitudes between 5 and 15 mV (rms). Each electrochemical measurement was repeated at least three times. For the EIS data modeling and curve-fitting method, NOVA impedance software was used. Mott-Schottky analysis was carried out on passive films at a frequency of 1 kHz using a 10 mV ac signal, and a step rate of 25 mV in the cathodic direction.

Table 1. Chemical compositions of AISI 420 stainless steel (wt.%)

Elements	Cr	Ni	Mo	Mn	Si	C	P	Cu	S	Fe
AISI 420	12.5	0.16	0.01	0.47	0.38	0.24	0.02	0.09	<0.003	Bal

3. Results and discussion

3.1. Open circuit potential (OCP) measurements

In Fig. 1, changes in the OCP of AISI 420 in H_2SO_4 solutions are shown. At the start of the immersion, the potential was immediately reduced, showing the dissolution of the oxide layer for all solutions. However, as time passed, the open circuit potential was directed towards the positive amount. This trend has also been reported for austenitic stainless steels in acidic solutions, thereby indicating the formation of the passive film and its role in increasing the protectivity with time. Fig. 1 also indicates that within an hour, a complete stable condition was achieved and electrochemical tests were possible.

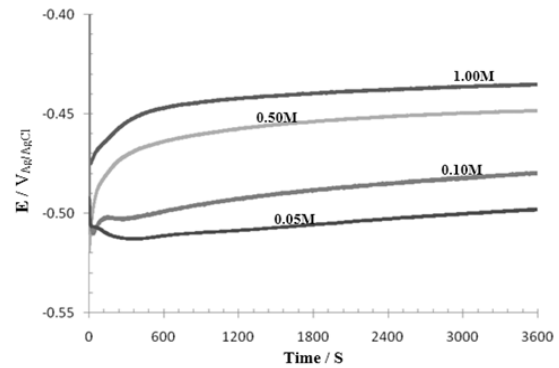


Fig.1. Open circuit potential plots of AISI 420 in H_2SO_4 solutions.

was transferred to a passive state, an active current peak occurred that could be related to the oxidation of Fe^{2+} to Fe^{3+} ions in the passive film^{23,24}.

The corrosion potential and corrosion current density at different concentrations of H_2SO_4 solutions for AISI 420 are summarized in Table 2. It can be observed from Fig. 2 and Table 2 that the corrosion potentials were shifted slightly towards the negative potential with the decrease in solution concentration. Also, the results showed that the corrosion current density was decreased with the decrease in the concentration of H_2SO_4 solutions.

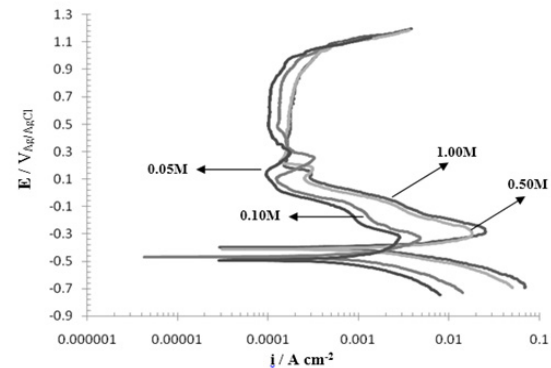


Fig.2. Potentiodynamic polarization curves for AISI 420 in H_2SO_4 solutions with different concentration.

Table 2. Corrosion potential and corrosion current density of potentiodynamic polarization obtained from AISI 420 in H_2SO_4 solutions.

H_2SO_4 Solutions	Corrosion potential ($V_{Ag/AgCl}$)	Corrosion current density ($A cm^{-2}$)
1.00 M	-0.409	3.3×10^{-3}
0.50 M	-0.422	2.6×10^{-3}
0.10 M	-0.473	9.4×10^{-4}
0.05 M	-0.497	6.1×10^{-4}

3.3. Mott-Schottky analysis

The outer layer of passive films contains the space charge layer and sustains a potential drop across the film. The charge distribution at the semiconductor/solution is usually determined based on Mott-Schottky relationship by measuring electrode capacitance, C , as a function of electrode potential (E)²⁵⁻²⁸:

$$\frac{1}{C^2} = \frac{2}{\varepsilon\varepsilon_0eN_D} \left(E - E_{FB} - \frac{kT}{e} \right) \text{ for n-type semiconductor (1)}$$

$$\frac{1}{C^2} = -\frac{2}{\varepsilon\varepsilon_0eN_A} \left(E - E_{FB} - \frac{kT}{e} \right) \text{ for p-type semiconductor (2)}$$

where e is the electron charge (-1.602×10^{-19} C), N_D is the donor density for n-type semiconductor (cm^{-3}), N_A is the acceptor density for p-type semiconductor (cm^{-3}), ε is the dielectric constant of the passive film (usually taken as 15.6), ε_0 is the vacuum permittivity (8.854×10^{-14} F cm^{-1}), k is the Boltzmann constant (1.38×10^{-23} J K^{-1}), T is the absolute temperature and E_{FB} is the flat band potential. Flat band potential can be determined from the extrapolation of the linear portion to $C^{-2} = 0$ ²⁵⁻²⁸.

Fig. 3 shows the Mott-Schottky plots of AISI 420 in H_2SO_4 solutions. Firstly, it should be noted that for all concentrations, capacitances were clearly increased with solution concentration. Secondly, all plots showed three regions in which a linear relationship between C^{-2} and E could be observed from them. The negative slopes in region I could be attributed to p-type behavior, probably due to the presence of Cr_2O_3 and FeO in the passive films²⁹. Region II presented positive slopes, which depicted an n-type semiconducting behavior. Finally, the negative slopes in region III could be attributed to p-type behavior, with a peak at around 0.7 and 0.75 V. This feature is usually explained in terms of the strong dependence of the Faradaic current on potential in the transpassive region. In this regard, the behavior of capacitance at high potentials near the transpassive region would be attributed to the development of an inversion layer as a result of increasing the concentration in the valence band²⁹.

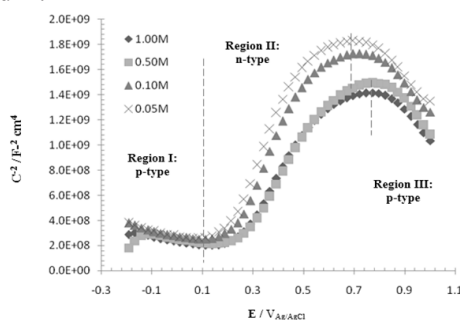


Fig.3. Mott-Schottky plots of AISI 420 in H_2SO_4 solutions. The electrodes were immersed at OCP for 1 h to form a steady-state passive film.

Also, in all plots, straight lines with negative and positive slopes were separated by a narrow potential plateau region, where the flat band potential (E_{fb}) was observed. For the potential more than 0.1 V, the positive slope indicated n-type behavior and for potentials less than 0.1 V, the negative slope represented the p-type behavior. Thus, Mott-Schottky analysis showed that the passive films formed on this stainless steel behaved as n-type and p-type semiconductors above and below the flat band potential, respectively. This behavior implied that the passive films had a duplex structure which would not have been realized if the measurements had been restricted to only anodic potentials. Early studies of the bipolar duplex structures of passive films on stainless steels were done by Sato³⁰, and followed by Ferreira et al, and Oguzie et al.^{31,32}. It has been well established that the inner part of the passive film, which has a p-type behavior, consists mainly of Cr oxides, while the outer region, with an n-type behavior, predominantly consists of Fe oxides. The p-type behavior, at $E < E_{fb}$, is related to the inner Cr oxide layer. There were negligible contributions from the Fe oxides in the outer part of the film, whereas the n-type behavior, at $E > E_{fb}$, was exclusively related to the outer Fe oxide region, with no contribution from the Cr oxide region³³.

According to Eqs. (1) and (2), donor and acceptor densities were determined by positive and negative slopes in regions II and III. Table 3 shows the calculated donor and acceptor densities for AISI 420 in H_2SO_4 solutions. The orders of magnitude were around 10^{21} cm^{-3} and therefore, comparable to those reported in other studies³⁴.

Table 3. Calculated donor and acceptor densities of passive films formed on AISI 420 in H_2SO_4 solutions as a function of concentration.

H_2SO_4 Solutions	Donor densities (cm^{-3})	Acceptor densities (cm^{-3})
1.00 M	2.692×10^9	6.902×10^9
0.50 M	2.633×10^9	6.089×10^9
0.10 M	1.916×10^9	3.529×10^9
0.05 M	1.796×10^9	3.502×10^9

According to Table 3, the donor and acceptor densities were increased with solution concentration. Changes in donor and acceptor densities corresponded to non-stoichiometry defects in the passive films. Therefore, it can be concluded that the passive film on AISI 420 was disordered. Based on the Point Defect Model (PDM)^{33,35}, the donors or acceptors in semiconducting passive layers were point defects. The PDM postulates that point defects present in a passive

film are cation vacancies, oxygen vacancies, and cation interstitials. Cation vacancies are electron acceptors, thereby doping the barrier layer p-type, whereas oxygen vacancies and metal interstitials are electron donors that result in n-type doping.

For the pure metals, the passive film is essentially a highly doped, defect semiconductor, as demonstrated by Mott-Schottky analysis. Not unexpectedly, the situation with regard to alloys is more complicated than that for the pure metals; this is because the substitution of other metal cations having oxidation states different from the host on the cation sublattice may also impact the electronic defect structure in the film.

According to the PDM, the flux of oxygen vacancy and/or cation interstitials (Cr^{2+} , Cr^{3+} , and Fe^{2+}) through the passive film is essential to the film growth process. In this study, the dominant point defects in the passive film at the low potential passive region were considered to be oxygen vacancies and/or cation interstitials acting as electron donors.

3.4. EIS measurements

Fig. 4 presents Nyquist plots obtained for the AISI 420 at OCP after 1 h immersion in H_2SO_4 solutions. As can be seen, Nyquist plots in both solutions showed a capacitive loop at high frequencies and an inductive loop at low frequencies. The high frequency capacitive loop could be assigned to the charge transfer of the corrosion process and the formation of oxide layer, while the low frequency inductive loop could be related to the relaxation process obtained by adsorption and incorporation of sulphate ions on and into the oxide film.

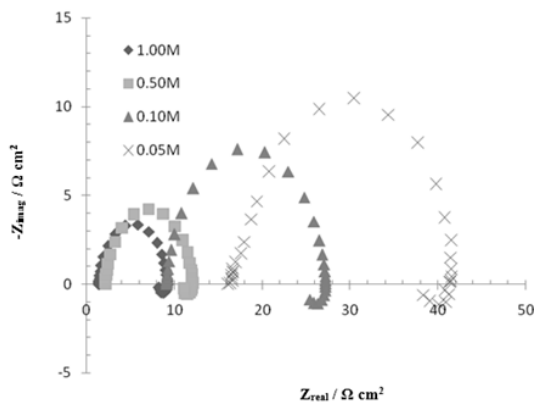


Fig.4. Nyquist plots of AISI 420 in H_2SO_4 solutions. The electrodes were immersed at OCP for 1 h.

The equivalent circuit shown in Fig. 5 was used to simulate the measured impedance data on AISI 420 in H_2SO_4 solutions.

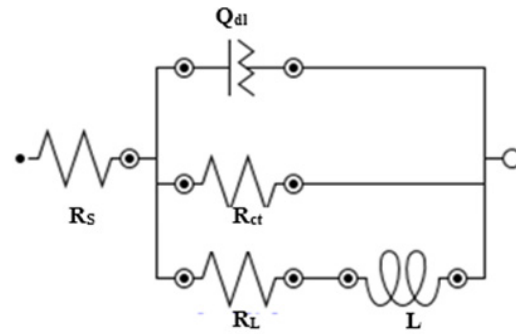


Fig.5. The best equivalent circuit used to model the experimental EIS data.

This equivalent circuit consists of a constant phase element (Q_{dl}) in parallel with parallel resistors R_{ct} (charge transfer resistance) and R_L (inductance resistance), which are in series with the inductor L . In this equivalent circuit, the polarization resistance (R_p) can be calculated from Equation 3³⁶⁾:

$$R_p = (R_{ct} \times R_L) / (R_{ct} + R_L) \quad (3)$$

As shown in Fig. 6, this equivalent circuit could fit the impedance data. Table 4 presents the best fitting parameters obtained for the films formed on AISI 420 immersed in 1.00, 0.50, 0.10 and 0.05 M H_2SO_4 solutions.

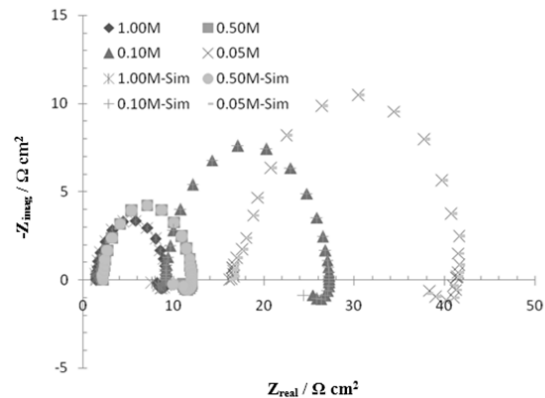


Fig.6. The fitting results of typical Nyquist plots of AISI 420 in H_2SO_4 solutions

As shown in Table 4, the fitting parameters R_{ct} and Y_{0dl} were affected by solution concentration. R_{ct} was higher, while the admittance of Q_{dl} seemed to be very close to the values expected for the double layer capacitance. Fitting data showed that as the concentration was decreased, the charge transfer resistance was increased.

It can be seen from Table 4 that the measured value of polarization resistance was increased with decreasing the concentration of the acid, thereby indicating that the corrosion current densities were decreased with the decrease in the concentration of H_2SO_4 solutions.

These results were in agreement with those obtained from potentiodynamic polarization.

Table 4. Best fitting parameters for the impedance spectra of AISI 420 in H₂SO₄ solutions.

H ₂ SO ₄ Solutions	RS (Ω cm ²)	CPE _{dl} (μΩ ⁻¹ cm ⁻² s ⁻ⁿ)	n _{dl}	R _{ct} (Ω cm ²)	R _L (Ω cm ²)	L (H)	χ ²	R _p (Ω cm ²)
1.00 M	1.37	743	0.91	7.86	52.1	160	0.0131	6.83
0.50 M	2.14	729	0.89	9.97	74.5	334	0.0136	8.79
0.10 M	9.05	460	0.89	18.2	128	368	0.0531	15.96
0.05 M	17.1	386	0.88	25.1	192	410	0.0315	22.21

4. Conclusions

1. The OCP plots showed that the open circuit potential was shifted towards positive amounts, indicating the formation of passive films.
2. The potentiodynamic polarization curves showed that corrosion current densities were decreased with the decrease in the concentration of H₂SO₄ solutions.
3. EIS studies showed that as concentration was decreased, the measured value of polarization resistance was increased. This trend was due to the decrease in the corrosion current density, which was in accordance with potentiodynamic polarization curves.
4. Mott–Schottky analysis showed the existence of a duplex passive film structure composed of two oxide layers of distinct semiconductivities (n-type and p-type). Also, based on the Mott–Schottky analysis, it was shown that donor and acceptor densities were in the order of 10²¹ cm⁻³, which was increased with solution concentration.

References

- [1] C.A. Gervasi, C.M. Méndez, P.D. Bilmes, C.L. Llorente: Mater. Chem. Phys., 126 (2011), 178.
- [2] C.A. Gervasi, P.D. Bilmes, C.L. Llorente, Metallurgical factors affecting localized corrosion of low-C 13CrNiMo martensitic stainless steels, I.S. Wang, Corrosion Research Trends, Nova Science Publishers, NY, (2007).
- [3] P.D. Bilmes, C.L. Llorente, C.M. Méndez, C.A. Gervasi: Corros. Sci., 51 (2009), 876.
- [4] D. Thibault, P. Bocher, M. Thomas: J. Mater. Process. Tech., 209 (2009), 2195.
- [5] X.P. Ma, L.J. Wang, C.M. Liu, S.V. Subramanian: Mater. Sci. Eng. A., 539 (2012), 271.
- [6] T. Ohtsuka, H. Yamada: Corros. Sci., 40 (1998), 1131.
- [7] J.S. Kim, E.A. Cho, H.S. Kwan: Corros. Sci., 43 (2001), 1403.
- [8] N. Le Bozec, C. Compère, M. L'Her, A. Laouenan, D. Costa, P. Marcus: Corros. Sci., 43 (2001), 765.
- [9] N.E. Hakiki, M. Da Cunha Belo, A.M.P. Simões, M.G.S. Ferreira: Electrochem. Soc., 145 (1998), 3821.
- [10] M. Da Cunha Belo, N.E. Hakiki, M.G.S. Ferreira: Electrochim. Acta., 44 (1999), 2473.
- [11] K. Sugimoto, Y. Sawada: Corros. Sci., 17 (1997) 425.
- [12] M.F. Montemor, A.M.P. Simões, M.G.S. Ferreira, M. Da Cunha Belo: Corros. Sci., 41 (1999), 17.
- [13] J. Amri, T. Souier, B. Malki, B. Baroux: Corros. Sci. 50 (2008), 431.
- [14] S. Ningshen, U. K. Mudali, V.K. Mittal, H.S. Khatak: Corros. Sci. 49 (2007), 481.
- [15] A.M.P. Simões, M.G.S. Ferreira, B. Rondot, M. da Cunha Belo: J. Electrochem. Soc., 137 (1990), 82.
- [16] I. Olefjord, L. Wegrelius: Corros. Sci., 31 (1990), 89.
- [17] S. Mischler, A. Vogel, H. Mathieu, D. Landolt: Corros. Sci., 32 (1991), 925.
- [18] M.F. Montemor, M.G.S. Ferreira, N.E. Hakiki, M. Da Cunha Belo: Corros. Sci. 42 (2000), 1635.
- [19] C. Sunseri, S. Piazza, F. Di Quarto, Photocurrent Spectroscopic Investigations of Passive Films on Chromium, J. Electrochem. Soc. 137 (1990), 2411.
- [20] M.J. Carmezim, A.M. Simões, M.O. Figueiredo, M. Da Cunha Belo: Corros. Sci., 44 (2002), 451.
- [21] S. Haupt, H.-H. Strehblow: Corros. Sci., 37 (1995), 43.
- [22] M.V. Cardoso, S.T. Amaral, E.M.A. Martini: Corros. Sci., 50 (2008), 2429.
- [23] K. Azumi, T. Ohtsuka, N. Sata: J. Electrochem. Soc., 134 (1987), 1352.
- [24] D.D. Macdonald, K.M. Ismail, E. Sikora: J. Electrochem. Soc. 145 (1998), 3141.
- [25] Y.X. Qiao, Y.G. Zheng, W. Ke, P.C. Okafor: Corros. Sci. 51 (2009), 979.
- [26] Y. Yang, L.-j. Guo, H. Liu: J. Power Sources 195 (2010), 5651.
- [27] Y.F. Cheng, C. Yang, J.L. Luo: Thin Solid Films.,

416 (2002), 169.

[28] N. Li, Y. Li, S. Wang, F. Wang: *Electrochim. Acta.*, 52 (2006), 760.

[29] C. Escrivà-Cerdán, E. Blasco-Tamarit, D.M. García-García, J. García-Antóna, A. Guenbour: *Electrochim. Acta*, 80 (2012), 248.

[30] N. Sato: *Corros. Sci.*, 31 (1990), 1.

[31] M.G.S. Ferreira, N.E. Hakiki, G. Goodlet, S. Faty, A.M.P. Simões, M. Da Cunha Belo: *Electrochim. Acta.*, 46 (2001), 3767.

[32] E.E. Oguzie, J. Li, Y. Liu, D. Chen, Y. Li, K. Yang, F. Wang: *Electrochim. Acta.*, 55 (2010), 5028.

[33] D.D. Macdonald: *J. Electrochem. Soc.*, 153 (2006), B213.

[34] A. Fattah-alhosseini, M.A. Golozar, A. Saatchi, K. Raeissi: *Corros. Sci.*, 52 (2010), 205.

[35] D.D. Macdonald: *J. Nuclear Materials.*, 379 (2008), 24.

[36] G.M. Pinto, J. Nayak, A.N. Shetty: *Int. J. Electrochem. Sci.*, 4 (2009), 1452.